Nucl. Sci. and Tech., Vol.11, No. 1 (2021), pp. 35-47

Nuclear Science and Technology

Journal homepage: https://jnst.vn/index.php/nst

Evaluation of the effect of filters on reconstructed image quality from cone beam CT system

Bui Ngoc Ha[1], Bui Tien Hung[], Tran Thuy Duong[1], Tran Kim Tuan[1], Tran Ngoc Toan[2]

[1]*Hanoi University of Science and Technology*
[2]*Vietnam Atomic Energy Institute*
Email: ha.buingoc@hust.edu.vn

Abstract: 3D Filtered Back Projection (FBP) is a three-dimensional reconstruction algorithm usually used in Cone Beam Computed Tomography (CBCT) system. FBP is one of the most popular algorithms due to its reconstruction is fast while quality of the result is acceptable. It can also handle a more considerable amount of data with same computer performance with other algorithms. However, the quality of a reconstructed image by the FBP algorithm strongly depends on spatial filters and denoising filters applied to projections. In this paper an evaluation of the reconstructed image quality of the CBCT system by using different denoising filters and spatial filters to find out the best filters for the CBCT system is performed. The result shows that, there is a significantly decrease of the noise of projection with the combination of Median and Gaussian filters. The reconstructed image has high resolution with Cosine filter and becomes more sharpen with Hanning filter.

Keywords: *Cone-Beam CT, FBP, filter, reconstruction.*

I. INTRODUCTION

Cone-Beam Computed Tomography (CBCT) is a transmission tomography technique, first used in medical imaging diagnostic in 1990 [1], with many advantages in object inspection. Therefore, in recent years, CBCT has been developed for industrial applications such as None-Destructive Testing (NDT), industrial object metrology [3,4]. Due to the development of radiation detection, mechanical engineering, and information technology, the CBCT's image had remarkable improvement in contrast and spatial resolution.

Today, the modern CBCTs usually use an X-ray generator with a focal spot size of only around a few micrometers. Flat Panel Detector (FPD) has a pixel size smaller than 200 micrometers. This configuration allows modern CBCT scanner to inspect very fine and complex samples with reconstructed images having spatial resolution in micrometer scale. CBCT has been commonly used for industrial applications in the inspection and metrology research of models such as casting objects, plane's components, electronic printed board, and lithium battery. CBCT can be used to analyze material density, inspect none surface defect that cannot be performed by other scanning methods [2,4].

Follow the improvement of CBCT's hardware, reconstruction algorithms have been quickly developed to produce high quality reconstructed images, reduce reconstruction time. There are several algorithms that are usually used in CBCT technic such as Filtered Back Projection (FBP), Algebraic Reconstruction Technique (ART), Simultaneous Iterative Reconstruction Technique (SIRT), Iterative Least-Squares Technique (ILST). FBP is an

https://doi.org/10.53747/jnst.v11i1.130
Received 28 October 2020, accepted 17 December 2020

essential algorithm for practical CBCT due to its simplicity and parallel computing capability; It also produces a high-quality image if the step angle between two adjacent projections is small enough [5-8]. The quality of reconstructed images by FPB depends strongly on a spatial filter, applied to projections; a suitable filter can reduce artifact and increase contrast of imaging, while a bad filter can cause some losses of imaging detail. Besides, the quality of reconstructed images also depends on the quality of FPD. In order to reduce the fluctuation of detectors in FPD and enhance the quality of projection data, a regular FPD calibration and a denoising filter to projections should be applied before performing filtered back projection. [9-11].

In this research, two sets of projection data are used. The first set were acquired by a BKCT-01 system (named BKCT-01), the second set were simulation data of this system by MCNP code. The reconstruction process was performed in two steps: the preprocessing that uses denoising filtering to projection, and the FBP that uses spatial filter and back-project. The best filters for BKCT-01 system were defined by assessing of reconstructed image.

II. CONTENT

A. Subject

In this study, a CBCT system, named BKCT-01 was used. The spatial resolution of whole system is up to 100~200 µm. Table I shows detailed configurations of the BKCT-01.

Table I. Configuration of BKCT-01 system

CBCT Gantry	Source to Detector Distance (SDD): 993 mm		
	Object to Detector Distance (ODD): 841 mm		
	Sample rotation: from 0 to 360^o with angle step is 0.5^o		
X-ray Source	X-ray energy: 0 – 240 kV		
	X-ray intensity: 0 – 3 mA		
	Spot size: 4 µm		
Matrix detector FPD		Normal mode	Binning mode
	Imaging size (pixel)	2944x2352	1472x1176
	Pixel pitch	49 µm	99 µm
	Resolution	10.1 LP/mm	5.0 LP/mm
	Framerate	8 fps	32 fps
	Digital converter	14 bits	14 bits

Reconstructed images of an aluminum sample obtained by BKCT-01 are used for investigating the effect of filters. The shape of the sample is a tiered cylinder with an internal diameter of 28 mm, the three-step cylinder has a thickness of 5 mm, and the diameter is 32, 34, and 36 mm, respectively. The information of sample is shown in figure 1 with the machining tolerance of 50 µm.

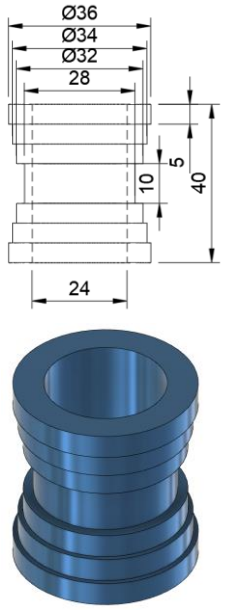

Fig. 1. Dimension of Aluminum sample in mm

Mechanical tolerance of real sample and fluctuation of FPB itself can cause error to the result. Therefore, a CBCT system (and sample) which is same configurations with BKCT-01 system was simulated using MCNP code. Projection data in both experiment and simulation include 720 projections over 360^o scanning angle; step angle is 0.5^o. FPD in CBCT system was working in normal mode. Projection datasets are preprocessed by applying denoising filters and then reconstructed using the FBP algorithm. By comparison results from the experiment and simulation, the best filter for the reconstruction of BKCT-01 by using the FBP algorithm can be found.

B. Methods

As mentioned above, the projection datasets undergo two processing steps to obtain 3D reconstructed images: preprocessing and filtered back projection. In the preprocessing step, each projection is applied to a denoising filter to reduce the statistical fluctuation of FPD. In the FBP step, projections are applied to the spatial filter and then back project to produce reconstructed images.

• ***Denoising filters***

In this paper, to eliminate the effect of FPD's statistical fluctuation, two denoising filters: Median filter and Gaussian filter are used. Median and Gaussian kernel is presented in Table II [12].

Table II. Median and Gaussian kernel

Filter	Kernel
Median filter	$M = \frac{1}{m \times n}\begin{bmatrix} 1 & 1 & 1 & \dots & 1 \\ 1 & 1 & 1 & \dots & 1 \\ . & . & . & \dots & 1 \\ . & . & . & \dots & 1 \\ 1 & 1 & 1 & \dots & 1 \end{bmatrix}$
Gaussian filter	$g(x,y) = ce^{-\frac{\left(x^2+y^2\right)}{2\sigma^2}}$

Where, m and n are width and height of kernel matrix, respectively; c is constant and σ is the standard deviation of the Gaussian distribution.

• ***Spatial filters***

The spatial filter is the most crucial factor that decides the quality of the reconstructed image from the FBP algorithm. In this paper, spatial filters were designed in the frequency domain to reduce artifact; the filtering stage is also done in the frequency domain, and then filtered projections are converted back to a spatial domain for the back projection state. Filtered back projection is described as below [13]:

$$g(t,s,z)=\int_0^{2\pi}\frac{D_{SO}^2}{(D_{SO}-s)^2}Q_\beta\left(\frac{D_{SO}t}{D_{SO}-s},\frac{D_{SO}z}{D_{SO}-s}\right)d\beta \quad (1)$$

With: $g(t,s,z)$ is a 3D reconstructed image of a sample in rotating coordinates (t,s,z), which is interpolated from Cartesian coordinates (x,y,z).:

$$\begin{bmatrix}t\\ s\\ z\end{bmatrix}=\begin{bmatrix}1 & 0 & 0\\ 0 & \cos\gamma & \sin\gamma\\ 0 & -\sin\gamma & \cos\gamma\end{bmatrix}\begin{bmatrix}\cos\theta & \sin\theta & 0\\ -\sin\theta & \cos\theta & 0\\ 0 & 0 & 1\end{bmatrix}\begin{bmatrix}x\\ y\\ z\end{bmatrix} \quad (2)$$

D_{SO} is a distance from source to rotating center, β is a rotating angle of Object.

$Q_\beta\left(\frac{D_{SO}t}{D_{SO}-s},\frac{D_{SO}z}{D_{SO}-s}\right)$ is a 2D projection of sample at rotated angle β that is calculated from equation (3) with R'_β is unfiltered projection, and h(t,s) is a spatial filtering.

$$Q_\beta\left(\frac{D_{SO}t}{D_{SO}-s},\frac{D_{SO}z}{D_{SO}-s}\right)=R'_\beta\left(\frac{D_{SO}t}{D_{SO}-s},\frac{D_{SO}z}{D_{SO}-s}\right)*\frac{1}{2}h(t,s) \quad (3)$$

In this research, six spatial filters were used: Ram Lak, Shepp Logan, Cosine, Hann, Flattop, and Parzen for this research. These filters are applied to projections before the back projection stage; and then the best filters for BKCT-01 system was determined. Functions of filters are shown in Table III [10,11,13].

Table III. Spatial filtering function

Filter	Function
Ram Lak	$h_{Ramp}(\omega)=\begin{cases}\lvert\omega\rvert & \text{if } \lvert\omega\rvert<W\\ 0 & \text{otherwise}\end{cases}$
Shepp Logan	$h_{Shepp}(\omega)=\begin{cases}\lvert\omega\rvert\frac{\sin(\omega)}{\omega} & \text{if } \lvert\omega\rvert<W\\ 0 & \text{otherwise}\end{cases}$
Cosine	$h_{Cosine}(\omega)=\cos\left(\frac{\pi n}{N}-\frac{\pi}{2}\right)$ if 0 < n < N
Hann	$h_{Hann}(\omega)=0.5\left(1+\cos\left(\frac{2\pi n}{N}\right)\right)$ if 0 ≤ n ≤ N
Flattop	$h_{Falttop}(\omega)=0.21-0.41\cos\left(\frac{2\pi\omega}{N-1}\right)+0.27\cos\left(\frac{4\pi\omega}{N-1}\right)$ $-0.08\cos\left(\frac{6\pi\omega}{N-1}\right)+0.006\cos\left(\frac{8\pi\omega}{N-1}\right)$ if 0 ≤ n ≤ N
Parzen	$h_{Parzen}(\omega)=\begin{cases}1-6\left(\frac{\lvert\omega\rvert}{N/2}\right)^2+6\left(\frac{\lvert\omega\rvert}{N/2}\right)^3 & \text{if } 0\le\lvert\omega\rvert\le(N-1)/4\\ 2\left(1-\frac{\lvert\omega\rvert}{N/2}\right)^3 & \text{if } (N-1)/4\le\lvert\omega\rvert\le(N-1)/2\end{cases}$

In which: W is limiting frequency of sampling process: $W = \frac{1}{2t}$ with t is sampling interval so call pixel size of FPD, t = 49µm, N is number pixel of FPD along filtering line. From the FPD parameters, a natural response of six spatial filters for the BKCT-01 system can be designed, as shown in figure 2.

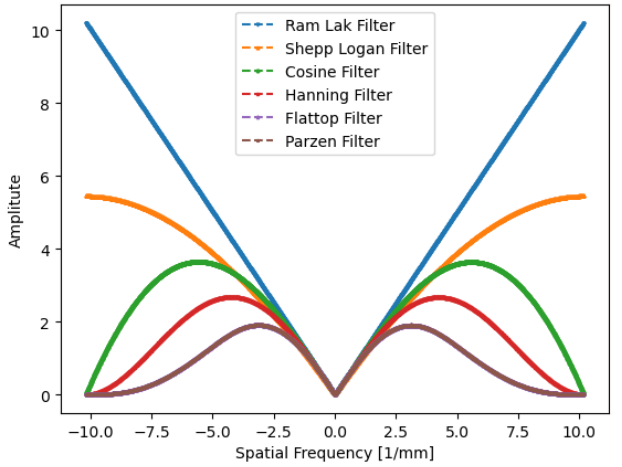

Fig. 2. Response of six different spatial filters is used in this paper

• ***Modulation transfer function (MTF)***

MTF of an imaging system is a measurement of its ability to transfer contrasts at a particular resolution from the Object to the image. MFT can show the limiting spatial resolution of the reconstructed image; for example, figure 3 shows the limiting spatial resolution at 10% modulation. MTF can be achieved by taking the Fourier transform of Line Spread Function (LSF) along the edge from a Region of Interest (ROI) as follows [2].

$$MTF = \left| \int_{-\infty}^{\infty} LSF(x) e^{-2\pi i f x} dx \right| \quad (4)$$

• ***Signal to Noise Ratio (SNR) and Contrast to Noise Ratio (CNR)***

The SNR and CNR ratio are used to measure the level of noise on ROI. This is a useful metric for describing an image's quality; the higher SNR and CNR, the better quality. The SNR and CNR are given by [2]:

$$SNR = \frac{\sum_i \left(x_i - \overline{x_{bg}} \right)}{\sigma_{bg}} \quad (5)$$

With: x_i is the gray value of ROI signal, $\overline{x_{bg}}$ is a mean background and σ_{bg} is a standard deviation of noise.

$$CNR = \frac{\left(\overline{x_s} - \overline{x_{bg}} \right)}{\sigma_{bg}} \quad (6)$$

With: $\overline{x_s}$ is an average gray value of ROI signal, $\overline{x_{bg}}$ is a mean background and σ_{bg} is a standard deviation of noise.

C. Result

• ***Quality of projections***

Figures 4a, 5a, and 6a show slices of projection those have abnormal areas. The irregular area is a negative peak at the position of column 45 in the image matrix. The gray level here drops to the very low level of 4500, without a denoising filter. After applying filters, this peak becomes shorter as shown in the previous figures, the larger the filter coefficients, the better remove the noise signal. Figures 4a, 5a, and 6a show the effect of kernel size on image sharpness. When the filter's

kernel size increases, the edge of the image becomes more inclined (Figure 4b, 5b, 6b), and this effect will reduce the spatial resolution of an image.

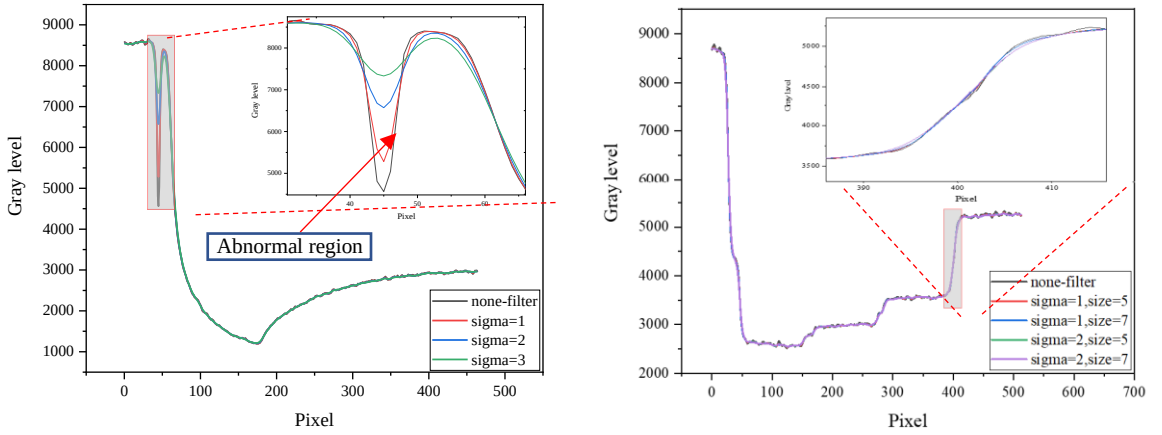

a) Vertical slice *b) Horizontal slice*

Fig. 4. Effect of Gaussian filter to horizontal and vertical slices at center of the projection

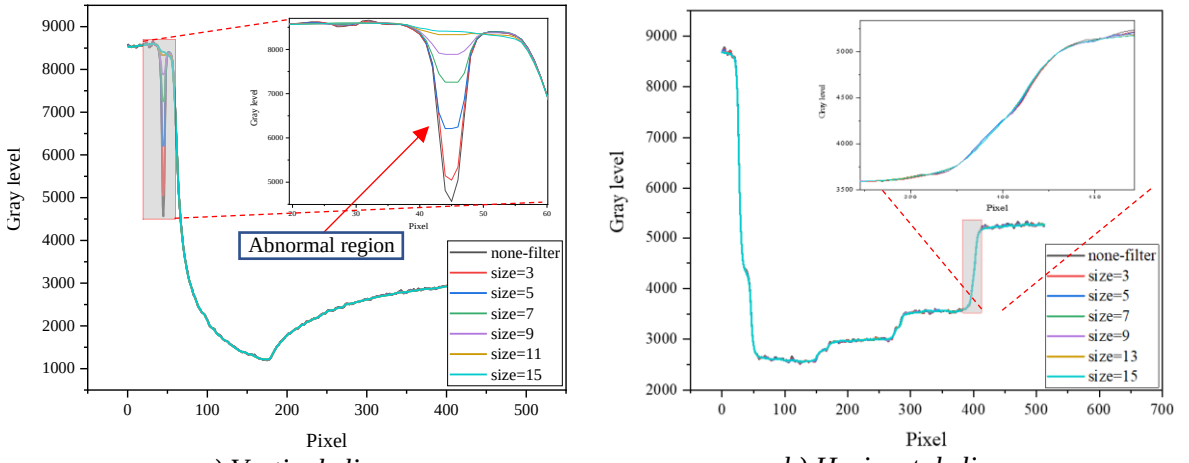

a) Vertical slice *b) Horizontal slice*

Fig. 5. Effect of Median filter to horizontal and vertical slices at center of the projection

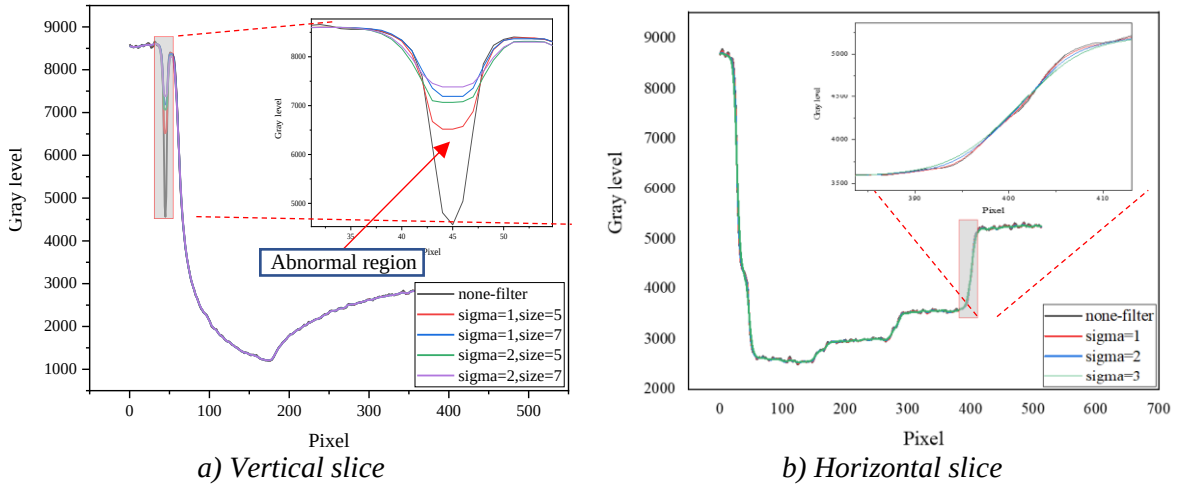

a) Vertical slice *b) Horizontal slice*

Fig. 6. Effect of Median filter combine with Gaussian to horizontal and vertical slices at center of the projection

Table IV shows the processing time for the denoising filter when applying to projection is shown, the processing time from 0.02 to 0.031 seconds for the Gaussian filter, and from 0.1 to 2.2 s for the median filter. The Median processing time is much larger than the Gaussian filter, and this time also increases with the filtering kernel size.

Table IV. Time to filter noise for one projection

Filter		**Time (s) per projection**
Gaussian	Sigma = 1	0.02
	Sigma = 2	0.03
	Sigma = 3	0.03
Median	S = 3x3	0.10
	S = 5x5	0.32
	S = 7x7	0.59
	S = 9x9	0.92
	S = 11x11	1.30
	S = 15x15	2.20

Since the quality of projections itself will affect the quality of reconstructed images, the noise level of projections has to be evaluated by using CNR and SNR values. The results are presented in Table V. When the filter's kernel size increases, CNR and SNR are better.

Table V. Results of the calculation of CNR and SNR ratio for the projection after filtering

Filter		**CNR**	**SNR**
Gaussian	Sigma = 1	147.71	20.90×10^6
	Sigma = 2	162.24	23.68×10^6
	Sigma = 3	180.20	24.57×10^6
Median	S = 5x5	153.41	21.91×10^6
	S = 7x7	160.83	23.38×10^6
	S = 9x9	166.65	24.77×10^6
	S = 11x11	171.40	26.17×10^6
	S = 15x15	180.11	0.14×10^6
Combine	Sigma = 1, s=5x5	157.61	22.84×10^6
	Sigma = 1, s=7x7	163.25	23.93×10^6
	Sigma = 2, s=5x5	165.55	24.60×10^6
	Sigma = 2, s=7x7	168.45	25.32×10^6

- ***Quality of reconstructed image***

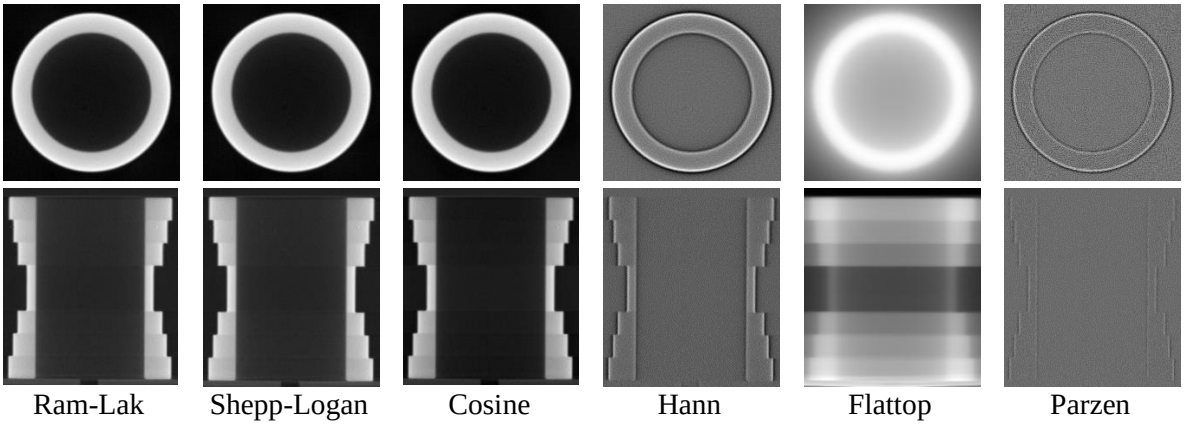

Fig. 7a. Object's reconstructed image with experimental projections

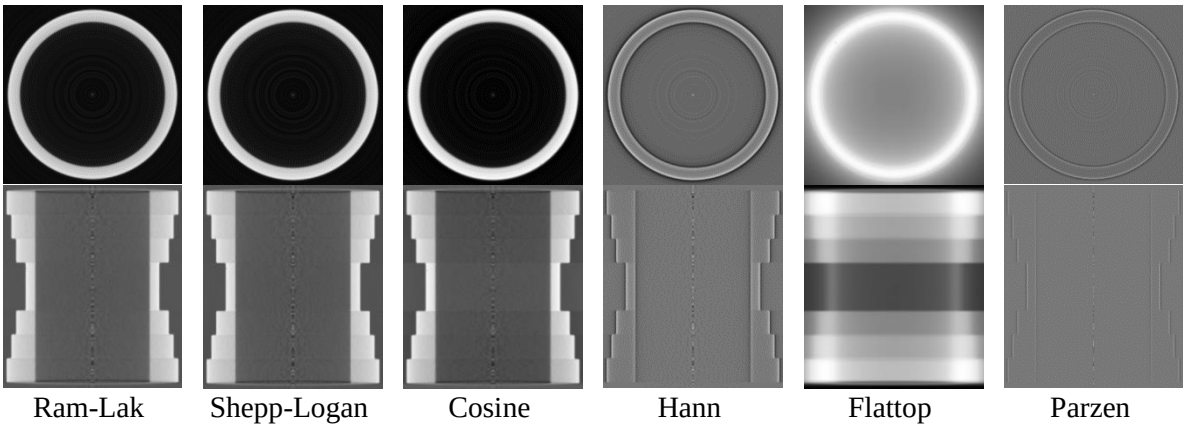

Fig. 7b. Object's reconstructed image with simulating projections

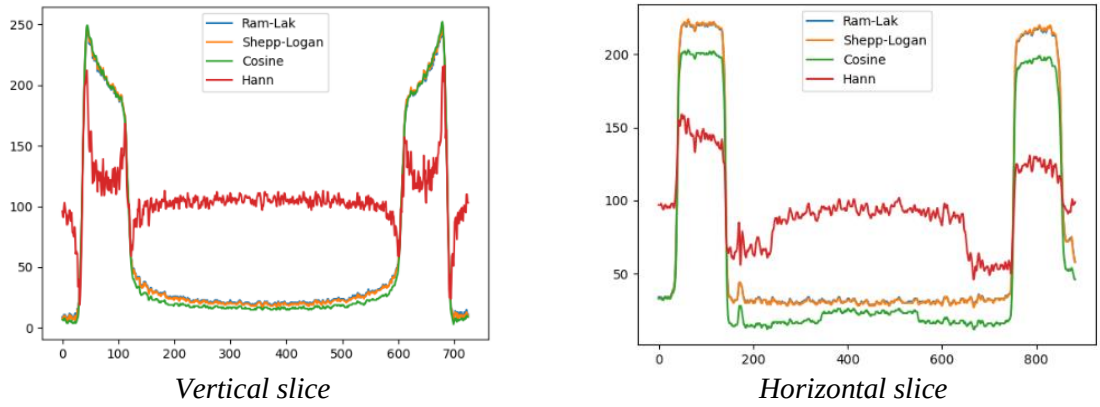

Fig. 8. Vertical and horizontal slice from Object's reconstructed image

Figure 7a and 7b show the horizontal and vertical slices of the reconstructed image. The actual object size does not change when using different types of filters. It can be seen that Ram-Lak, Shepp-Logan, and cosine filter generate similar results by observing with the naked eye. Hann and Parzen make a sharper image (detect edge only), while the result

achieved by applying the Flattop filter is blurry. For further analysis, a 1D curve of vertical-horizontal was plotted, as shown in Figure 8. The result shows that, by applying Cosine filter, a base level of signal drops closer to zero than by applying Ram-Lak and Shepp-Logan filter. In addition, when evaluating with SNR and CNR ratios (result in Table VI), Ram-Lak, Shepp-Logan, and Cosine filter gave relatively large values of CNR and SNR among the six filters used. While the Hann, Flattop, and Parzen filters have a meager CNR ratio, that can be seen clearly in the image with almost indistinguishable details in the area with the Object; only the edges are visible.

Table VI. Results of calculation of CNR and SNR ratio for reconstructed image

Filter		Ram-Lak	Shepp Logan	Cosine	Hann	Flattop	Parzen
CNR	Simulation	13.17	13.20	15.42	2.69	1.27	0.61
	Experiment	33.96	33.99	39.52	9.92	1.40	2.62
SNR	Simulation	1.86×10^6	1.89×10^6	2.20×10^6	3.85×10^5	1.83×10^5	8.78×10^4
	Experiment	4.73×10^6	4.73×10^6	5.50×10^6	1.38×10^5	1.95×10^5	3.65×10^5

• ***Modulation transfer function (MTF)***

Measure the intensity of reconstructed along the edge of a sample, the LSF of the image is shown in the following figure (figure 9).

The MTF of reconstructed image in different filter types was measured by taking the Fourier transform of LSF (figure 10). It is clear that, the contrast of result from Flattop filter quickly drops below 10% of modulation at around 1 LP/mm; Hann and Flattop caused low modulation at low frequency and then oscillated when frequency increases. Ram-Lak and Shepp-Logan have similar responses with limiting spatial resolution of 6 and 5.5 LP/mm for results from real sample and simulating sample, respectively. Cosine filter has limiting spatial resolution around 10LP/mm for both actual sample and simulating one.

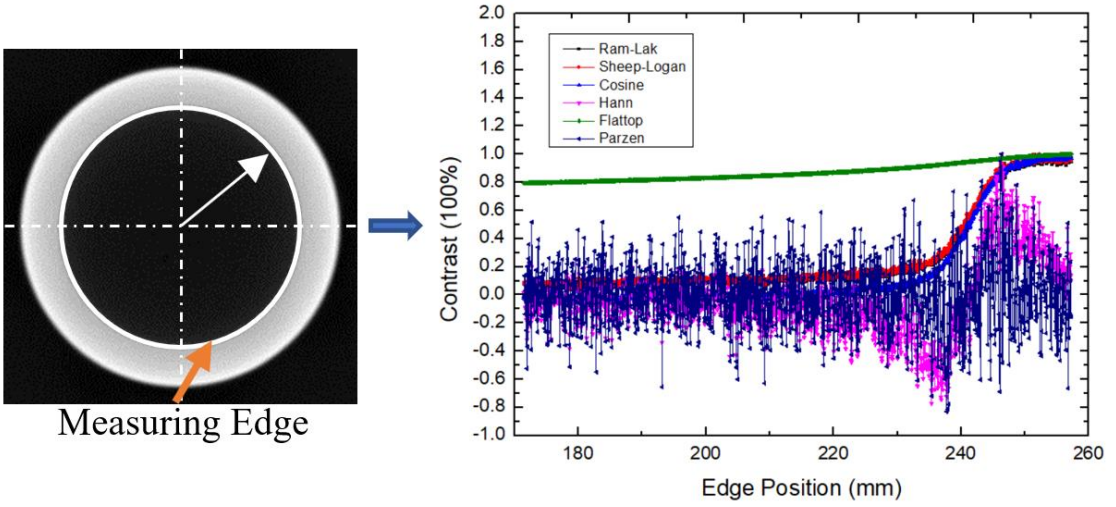

Fig. 9. LSF of reconstructed slide with difference filters

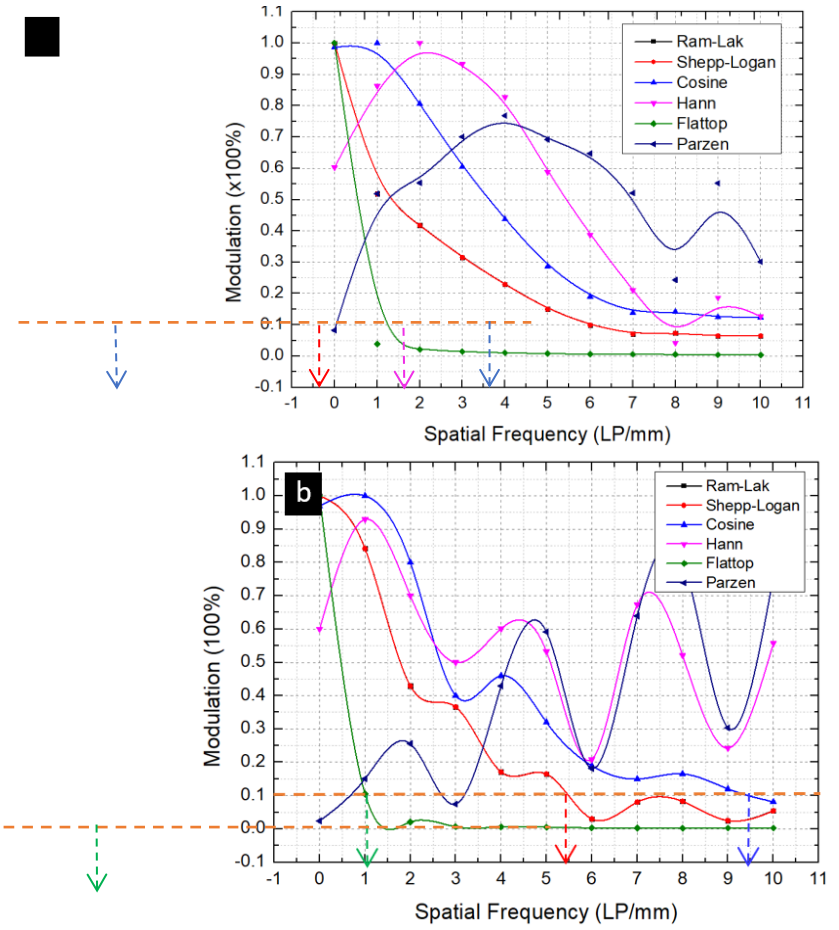

Fig. 10. Fitting functions of MTF of reconstrued image by applying six difference filters; (a): result from real sample, (b): result from simulating sample

• ***Calculation of Object's dimension***

To calculate the sample's dimension in both experimental and simulated cases, contours of Object were detected and measures in the reconstructed image, which are shown in Table VII. The calculated values show that the diameter of the Object is relatively accurate compared with the fabrication size of the specimen. The difference is less than the value of 2 pixels, which is smaller than 100 μm.

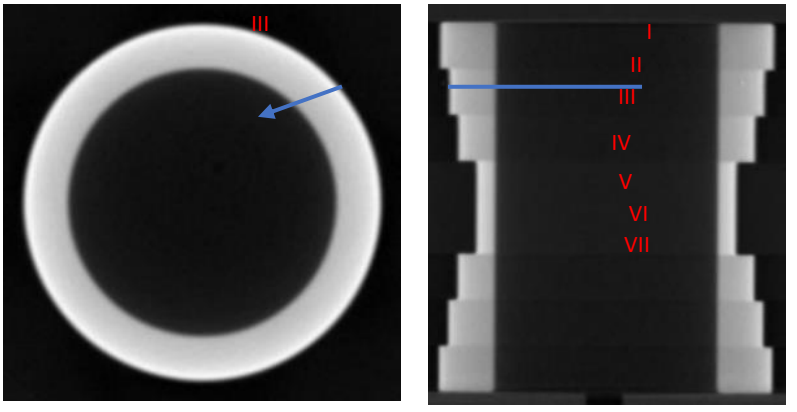

Fig. 11. Mark the dimension of the reconstructed image by applying Cosine filter

Table VII. Measurement of the Object's dimension

Slice	Actual size (mm)	Measuring size from reconstructed image (mm)	
		Experimental Sample	Simulating Sample
I	36 (±0.05)	35.929±0.081	35.988±0.077
II	34 (±0.05)	33.964±0.073	33.918±0.075
III	32 (±0.05)	32.000±0.075	31.962±0.075
IV	28 (±0.05)	28.084±0.075	28.060±0.078
V	32 (±0.05)	32.009±0.080	31.962±0.075
VI	34 (±0.05)	34.059±0.068	33.913±0.080
VII	36 (±0.05)	35.926±0.077	35.988±0.075

D. Discussion

Because of the detector system's instability, some abnormal regions were detected as shown in Figure 4a and Figure 5b. Fortunately, this problem could be solved by using Gaussian and Median filters. The larger the filter coefficients, the better the removal of the anomalous signal. The median function with a filter coefficient (Kernel matrix size) of 15x15 can reduce the signal's noise level better than the Gaussian filter. However, the problem is that too much filtering can lose information of the image, making the edge of the Object in the projections even more slopping, as shown in Figure 4b, 5b, and 6b. Therefore, the selection of a large filter coefficient needs to be carefully considered. It could be found that the use of the Median filter requires a greater computation time than the Gaussian filter (shown in Table IV). Therefore, we should not choose a Median filter with a large size such as 11x11 or 15x15, because when dealing with large number projections, the filtering process will take much time and then reduce computing performance.

The projections' quality will also affect the reconstructed image quality, so a further evaluation of the CNR and SNR ratio was implemented. The increase of filter coefficient will give better quality. However, as mentioned above, this increase could not be arbitrarily done because it will lose the edges of images' sharpness. Furthermore, with the resolution requirement, when using the filters, the image's spatial resolution will be decreased. The Median filter with a Kernel size of 7x7 will have a resolution of about 0.2 mm, while filtering with a Kernel size of 3x3 equivalent to a resolution of 0.05 mm is not enough. Therefore, a filtration scheme with a Sigma coefficient equal to 1 or 2 was proposed and the Median with Kernel size of 5x5 was used. The set of chosen filters can be expected to achieve results with a resolution around 0.1 mm.

The spatial resolution of the reconstructed image is measured in figure 10; the response of Ram-Lak, Shepp-Logan, cosine, Flattop in both experimental and simulated sampling is quite similar. In simulating the sample, the curve of these filters is a little bit oscillated of high frequency due to high-frequency noise, which is caused by statistical fluctuation when simulation time of

MCNP is not high enough. Reconstruction from projections of simulating sample will lead to spatial resolution of simulation results is slightly smaller than from experiment. Hann and Flattop filters have a smoother response at high frequency; therefore, they fluctuate strongly when the frequency is increased and may not be used in case of simulating sample.

Table VII shows the sample's dimension, which is calculated from the reconstructed image with a cosine filter; maximum machining tolerances of the real sample is 0.05 mm; tolerance does not appeal in the simulated sample. It can be seen that the maximum error of dimension does not exceed 0.1 mm; this corresponds to limiting spatial resolution, which is measured in figure 10.

III. CONCLUSIONS

In this paper, some denoising filters and spatial filters are used to evaluate the reconstructed image's quality from the cone-beam CT system. The results show that the denoising filter should be first applied for all projections in the preprocessing step because of the noise. The most suitable filter for the denoising process is a mixed of Gaussian and Median with the right kernel size. For the elimination of higher noise’s frequency in projections, a larger filter is needed, but a reduction in the reconstructed image's sharpening is appeared. The median filter has a better response than the Gaussian filter, but the Median's processing time is much slower than Gaussian. Therefore, the combination of these two filters is needed.

The spatial filter has a significant effect on the quality of the reconstructed image. From the results, it can be seen that the reconstructed image has the highest spatial resolution by applying a cosine filter. Limiting the spatial resolution of reconstructed data for both real simulation samples is around 10 LP/mm. It means that by applying a Cosine filter, the spatial resolution is 0.1 mm on the reconstructed image. Ram-Lak and Shepp-Logan filters have similar response with a limiting resolution is around 6 LP/mm. Hann and Parzen make images with low contrast at low frequency and increase at higher one, while Flattop makes image drop contrast quickly when frequency increases. Therefore, a cosine filter was chosen to achieve an image with high resolution and a wide range of contrast (having full information of the reconstructed sample). Nevertheless, to obtain a high frequency of images only, the edge of the Object in an image should be seen only; it means a Hann filter should be used in a segmentation application.

By evaluation of the effect of filter types on quality of reconstructed image when using FBP algorithm on CBCT system, a suitable filter for reconstruction of BKCT-01 system was chosen. The system can archive a good quality of the reconstructed image and then accurately measure the sampling object's dimension by Using the right set of filters.

ACKNOWLEDGMENTS

This research is supported by KC.05.18/16-20 Project of Ministry of Science and Technology and Vietnam Atomic Energy Institute via VINATOM-HPC system.

REFERENCES

[1]. Shaithya Kailash, "CBCT-Cone Beam Computed Tomography", Journal of Academy of Dental Education, 9-15, 2014.

[2]. Jerrold T. Bushberg, J. Anthony Seibert, Edwin M. Leidholdt JR, John M. Boone, "The essential physics of medical imaging", 3rd

edition, Lippncott William & Wilkins, p70-72, 91-92, 312-318, 2012.

[3]. J.P. Kruth, M. Bartscher, S. Carmignato, L. De Chiffre, A. Weckenmann, "Computed Tomography for dimensional metrology", CIRP Annals – Manufacturing Technology 60, 655-677, 2011.

[4]. L. De Chiffre, S. Carmignato, J.P. Kruth, R. Schmitt, A. Weckenmann, "Industrial application of Computed Tomography", CIRP Annals – Manufacturing Technology 63, 655-677, 2014.

[5]. Jia, X., Dong, B., Lou, Y., & Jiang, S. B., "GPU-based iterative cone-beam CT reconstruction using tight frame regularization", Physics in Medicine & Biology, 56(13), 3787, 2011.

[6]. Hsieh, J., Nett, B., Yu, Z., Sauer, K., Thibault, J. B., & Bouman, C. A., "Recent advances in CT image reconstruction", Current Radiology Reports, 1(1), 39-51, 2013.

[7]. Pack, J. D., Noo, F., & Clackdoyle, R., "Cone-beam reconstruction using the back projection of locally filtered projections", IEEE Transactions on Medical Imaging, 24(1), 70-85, 2005.

[8]. Scherl, H., Koerner, M., Hofmann, H., Eckert, W., Kowarschik, M., & Hornegger, J., Implementation of the FDK algorithm for cone-beam CT on the cell broadband engine architecture. In Medical Imaging 2007: Physics of Medical Imaging (Vol. 6510, p. 651058). International Society for Optics and Photonics, March 2007.

[9]. Mark Plachtovics, Janos Goczan, Katalin Nagy, "The effect of calibration and detector temperature on the reconstructed cone beam computed tomography image quality: a study for the workflow of the iCAT Classic equipment", Oral Surgery, Oral Medicine, Oral Pathology and Oral Radiology, Vol 119, Issue 4, p473-480, 2015.

[10]. Yuuki Houno, Toshimitsu Hishikawa, Ken-ichi Gotoh, Munetaka Naitoh, Akio Mitani, Toshihide Noguchi, Eiichiro Ariji, Yoshie Kodera, "Optimizing the reconstruction filter in cone-beam CT to improve periodontal ligament space visualization: An in vitro study", Imaging Science Density, 47(3):199-207, September 2017.

[11]. Julia F. Barrnet, Nicholas Keat, "Artifact in CT: Recognition and Avoidance", Radio graphic, 24, p1679-1691, 2004.

[12]. Linda G. Shapiro, George Stockman, "Computer Vision", University of Washington, p154-155,168, 2000.

[13]. Avinash C. Kak, Malcoim Slaney, "Principle of Computerized Tomographic Imaging", SIAM, p71-74,104-107, 1988.